

Statistical Theory of Plasmas Turbulence^{*)}

Eun-jin KIM and Johan ANDERSON

Department of Applied Mathematics, University of Sheffield, Sheffield, S3 7RH, U.K.

(Received 31 August 2008 / Accepted 20 April 2009)

We present a statistical theory of intermittency in plasma turbulence based on short-lived coherent structures (instantons). In general, the probability density functions (PDFs) of the flux R are shown to have an exponential scaling $P(R) \propto \exp(-cR^s)$ in the tails. In ion–temperature–gradient turbulence, the exponent takes the value $s = 3/2$ for momentum flux and $s = 3$ for zonal flow formation. The value of s follows from the order of the highest nonlinear interaction term and the moments for which the PDFs are computed. The constant c depends on the spatial profile of the coherent structure and other physical parameters in the model. Our theory provides a powerful mechanism for ubiquitous exponential scalings of PDFs, often observed in various tokamaks. Implications of the results, in particular, on structure formation are further discussed.

© 2009 The Japan Society of Plasma Science and Nuclear Fusion Research

Keywords: turbulence, structure, shear flow, confinement, probability density function (PDF)

DOI: 10.1585/pfr.4.030

1. Introduction

The need for statistical theory of plasma turbulence has grown significantly over the past decade with accumulating evidence from simulation and experiments showing highly intermittent and bursty turbulent transport [1–9]. Probability density functions (PDFs) inferred from these experiments are strongly non-Gaussian, particularly in the tails, due to rare events of large amplitude. For instance, exponential scalings appear to be a robust feature of the tails of heat, particle, and momentum fluxes in a variety of tokamaks (for example, [10–13]). These observations suggest that Gaussian statistics and average transport coefficients based on mean field theory fail to capture essential transport processes of intermittency and demand a proper nonlinear theory for events of large amplitude. Given the potentially disastrous impact of these events on confinement, the importance of a predictive theory of PDF tails cannot be overemphasized.

While these coherent structures mediate significant transport, as mentioned above, they can also play a complementary role in inhibiting transport via enhanced decorrelation. Improvements in plasma confinement by mean flows and zonal flows [14] are notable examples. Given the importance of such structures in intermittency and transport, the PDF of the formation of the structure itself is a quantity of ultimate interest. For instance, an interesting issue is the prediction of the PDF of the L→H transition [15].

This paper presents a non-perturbative theory of PDFs in plasma turbulence and investigates the structure formation — in particular, zonal flow formation. Our theory

is motivated by the following key experimental observations. The first is that coherent structures (which tend to form naturally in nonlinear systems) mediate fast transport and are responsible for the intermittency in the PDFs. The second is that coherent structures tend to be short-lived in time, causing bursty events (for example, [12, 13]). Examples of such short-lived structures include streamers, blobs, and vortices. This empirical fact that short-lived coherent structures are responsible for intermittency and PDF tails is precisely built into our theoretical tool: the so-called “instanton method.” Section 2 provides a few brief comments on the method. Sections 3 and 4 describe the use of this method to develop a non-perturbative theory of the PDFs of structure formation in the ion–temperature–gradient (ITG) model. Section 5 presents a discussion and conclusions.

2. Instantons

This section provides historic background on instantons to help readers understand their physical significance and why they are useful for the development of a statistical theory of turbulence. Instantons originated in quantum mechanics as a non-perturbative way of computing the transition amplitude from one ground state to another [16]. The basic idea is that the uncertainty relationship between position and momentum allows one to formulate the transition amplitude from the initial position x_i to the final position x_f by a path integral as follows (see Fig. 1):

$$\langle x_f | e^{iHT/\hbar} | x_i \rangle = N \int_{x=x_i}^{x=x_f} \mathcal{D}x(t) e^{iS/\hbar},$$

where $S = \int dt [mv^2/2 - U(x)]$ is action, and $H = mv^2/2 + U(x)$ is a Hamiltonian with potential U . We can expand the left side of the equation in terms of a complete set of

author's e-mail: e.kim@shef.ac.uk

^{*)} This article is based on the invited talk at the 14th International Congress on Plasma Physics (ICPP2008)

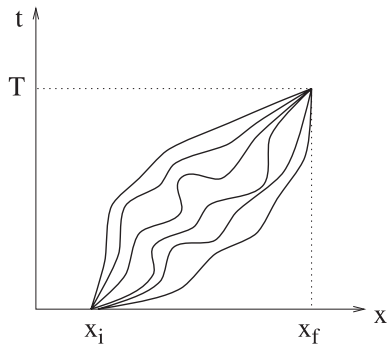


Fig. 1 Trajectories of a particle between initial position x_i at time $t = 0$ and final position x_f at $t = T$.

energy eigenstates to obtain

$$\langle x_f | e^{iHT/\hbar} | x_i \rangle = \sum_n \langle x_f | E_n \rangle \langle E_n | x_i \rangle e^{iE_n T/\hbar}.$$

The previous equation implies that the transition amplitude from one ground state to another can be isolated by taking time to be imaginary. Expressed in terms of imaginary time, action becomes “Euclidean action” $S_E = \int dt [mv^2/2 + U]$. An instanton is a saddle-point solution of Euclidean action and corresponds to one particular path that leads to the transition amplitude between ground states. For instance, in the case of double-well potential, an instanton is a tunneling solution from the bottom of one potential well to another (see Fig. 2 (a)). If a solution going from one ground state to the other is called an instanton, a solution traveling in the opposite direction is called an anti-instanton. As noted above, a distinguishing characteristic of such solutions is temporal localization (see Fig. 2 (b)). The instanton method was used in gauge field theory to compute the transition amplitude from one vacuum to another vacuum [17]. About 20 years later, the method was adapted to a classical fluid problem by several authors [18–21].

3. PDF Tails in Plasma Turbulence

Armed with general concepts of instantons, in this section, we develop a general theory of PDFs in plasma turbulence. In plasma turbulence, unpredictability can arise either from the chaos intrinsic to the system or from an external random forcing. Between the two, clearly, it is much easier to formulate a PDF in the case of an external forcing, to which the following discussion is limited. In fact, it is well known that a similar path integral can be formulated for stochastic equations with a random external forcing [22, 23]. For instance, the effective action for classical forced systems was formulated by Martin, Siggia, and Rose in 1973 [24]. However, the non-perturbative evaluation of a path integral had to wait until the (non-perturbative) saddle-point (instanton) method was used to compute the tail of the PDF [18, 19].

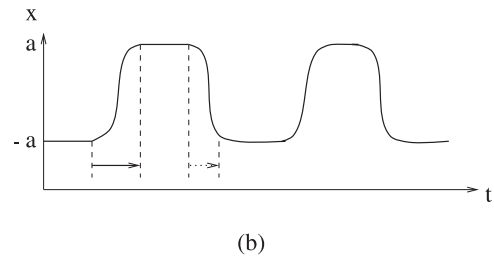
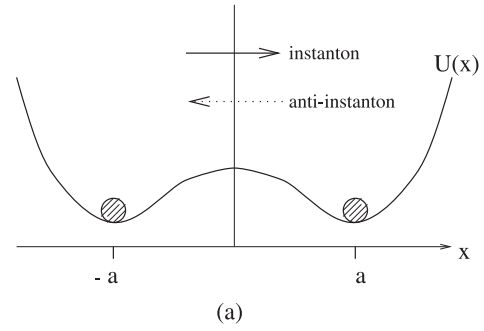


Fig. 2 (a) Double-well potential with a particle sitting at the bottom of a potential well. A particle going from $x = -a$ to a is an instanton; a particle going from $x = a$ to $-a$ is an anti-instanton. (b) Position of a particle as a function of time, traveling between $x = -a$ and a . The positive (negative) slope corresponds to an instanton (anti-instanton).

We consider a prototype nonlinear dynamical system driven by an external (stochastic) forcing f

$$\partial_t \phi + N(\phi) = f, \tag{1}$$

where $N(\phi)$ represents the sum of linear and nonlinear interactions with the highest nonlinearity of n . For simplicity, we take the statistics of the forcing in Eq. (1) to be Gaussian with delta-correlation in time as follows:

$$\langle f(\mathbf{x}, t) f(\mathbf{x}', t') \rangle = \delta(t - t') \kappa(\mathbf{x} - \mathbf{x}'), \tag{2}$$

and $\langle f \rangle = 0$. For Gaussian statistics with a vanishing first moment, the prescription for the second moment given by Eq. (2) is sufficient, simply because all odd moments vanish while even moments can be expressed as a product of second moments. Note that, even if the forcing is Gaussian, ϕ statistics can be non-Gaussian because of the nonlinearity of the dynamical equation. An equivalent way of prescribing the second moment (Eq. (2)) for the Gaussian forcing is to introduce the PDF of f as follows [23]:

$$d[\rho(f)] = \mathcal{D}f e^{-\frac{1}{2} \int dx dx' dt f(x, t) \kappa^{-1}(x, x') f(x', t)}. \tag{3}$$

This is a generalization of a Gaussian distribution to a continuous variable $f(\mathbf{x}, t)$. The average value of a quantity Q is then computed as

$$\langle Q \rangle = \int d[\rho(f)] Q, \tag{4}$$

where the angle brackets $\langle \rangle$ represent the average over the statistics of the forcing f . From Eq. (3), we construct the PDFs of flux, which are the m multiple products of ϕ (that is, the m th moment). In the following, we call $M(\phi)$ the “observable,” since we are interested in measuring its PDFs. The PDFs of $M(\phi)$ to take a value of R can then be represented in terms of a path integral as follows:

$$\begin{aligned} P(R) &= \langle \delta(M(\phi) - R) \rangle \\ &= \int d\lambda e^{i\lambda R} \langle e^{-i\lambda M[\phi]} \rangle \\ &= \int d\lambda e^{i\lambda R} I_\lambda, \end{aligned} \tag{5}$$

where

$$I_\lambda = \langle e^{-i\lambda M[\phi]} \rangle.$$

By taking $Q[\phi] = \exp[-i\lambda M[\phi]]$ in Eq. (4) and using Eq. (3), we can rewrite I_λ in terms of a path integral as

$$I_\lambda = \int \mathcal{D}\phi \mathcal{D}\bar{\phi} e^{-S_\lambda}, \tag{6}$$

where S_λ is the effective action given by

$$\begin{aligned} S_\lambda &= -i \int dx dt \bar{\phi} [\partial_t \phi + N(\phi)] \\ &+ \frac{1}{2} \int dx dx' dt \bar{\phi}(x) \kappa(x - x') \bar{\phi}(x') \\ &+ i\lambda \int dt M(\phi) \delta(t). \end{aligned} \tag{7}$$

In Eq. (7), $\bar{\phi}$ is the conjugate variable to ϕ , introduced to impose the constraint given by the equation of motion of ϕ in Eq. (1) in the form

$$N = \int D\bar{\phi} \exp \left\{ i \int dx dt \bar{\phi} [\partial_t \phi + N(\phi) - f] \right\},$$

with a normalization constant N . Although $\bar{\phi}$ appears to be simply a convenient mathematical tool, it does have a useful physical meaning: it arises from the uncertainty in the value of ϕ due to stochastic forcing. That is, the dynamical system with a stochastic forcing should be extended to a larger space involving this conjugate variable, whereby ϕ and $\bar{\phi}$ constitute an uncertainty relationship (see Fig. 3). The instanton solution is a particular path out of all possible (functional) values of ϕ and $\bar{\phi}$ which minimizes the action S_λ . Furthermore, the conjugate variables have the interesting physical property of mediating the forcing κ and the flux $M(\phi)$ (observable) whose PDFs are sought (see Fig. 4).

3.1 Instanton solution

The key concept underlying the instanton method is that coherent structures that are localized in time are responsible for the rare events of large amplitude, causing strong intermittency in the PDF tails with possibly significant transport. Assuming that such a coherent structure has a spatial profile $\phi_0(x)$ and a temporal evolution governed

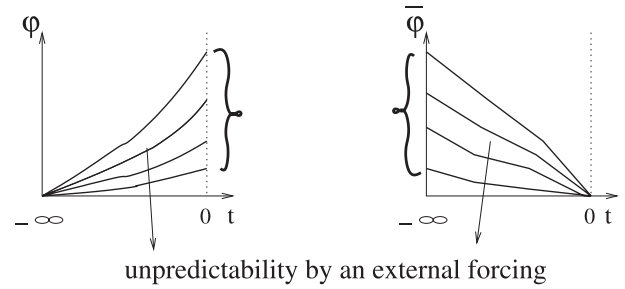


Fig. 3 Uncertainty in $\phi = F(t)\phi_0$ and $\bar{\phi} = \mu(t)\bar{\phi}$ (or in $F(t)$ and $\mu(t)$) due to stochastic forcing.

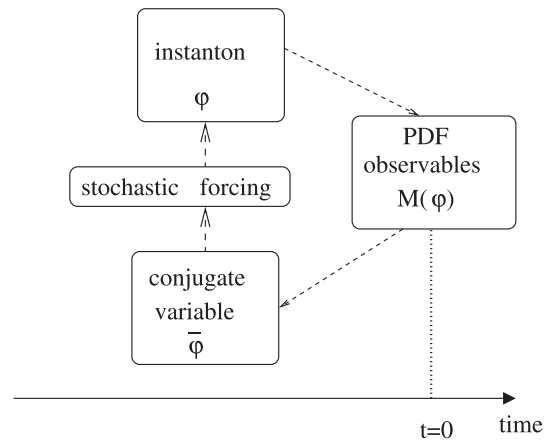


Fig. 4 Schematic diagram showing the relationship among the PDFs of the observable $M(\phi)$, dynamical quantity ϕ , its conjugate variable $\bar{\phi}$, and the stochastic forcing with the correlation function $\kappa(x - x')$ (see Eq. (2)).

by $F(t)$ as $\phi(x, t) = \phi_0(x)F(t)$, and similarly $\bar{\phi} = \bar{\phi}_0(x)\mu(t)$, we can rewrite the action S_λ and minimize it with respect to F and μ to obtain equations for F and μ . Since the instanton $\bar{\phi}$ propagates forward in time and its conjugate variable ϕ backward in time while the PDF is computed at $t = 0$, the boundary conditions on F and μ are (see also Fig. 3):

$$F(-\infty) = 0, \tag{8}$$

$$\mu(t > 0) = 0. \tag{9}$$

To make further progress, we need to specify the profile of ϕ_0 . The key question is thus “what should we use for ϕ_0 ?” or, alternatively, “what are the possible coherent structures that are likely to form in a given nonlinear system?” As noted previously, exact solutions to nonlinear equations that tend to be supported naturally are examples of such structures. In the presence of stochastic forcing, these structures can readily be created, being localized in time. Ramps in Burgers equations, and modons in Hasagawa-Mima and ITG turbulence models are examples of such coherent structures. In the presence of stochastic forcing, these structures are likely to form and decay with a short lifetime. By using the profiles of these structures

and expanding the correlation functions in terms of those as

$$\kappa(x-y) \sim \kappa_0 \sum_{m,n} \phi_0^m(x) \phi_0^n(y),$$

where κ_0 is the strength of forcing, we can, in principle, cast the action in terms of a time-integral only. Schematically, computation of the PDFs then requires the following main steps:

- I. Minimize S_λ with respect to μ and F to obtain the equation of motion for F and μ .
- II. Solve those equations with the boundary conditions (Eqs. (8) and (9)) to compute optimal paths.
- III. Use those solutions to obtain the minimum action S_λ .
- IV. Evaluate λ integral in Eq. (5) to find the PDFs.

4. PDFs of Structure Formation in ITG Turbulence

This section predicts the PDFs of structure formation in ITG turbulence by the preceding steps. As a specific example, we investigate the PDFs of the formation of zonal flows. Since zonal flows are self-driven from turbulence by Reynolds stress, this problem is closely related to the PDF of momentum flux. We thus consider the PDFs of momentum transport and zonal flow formation. The PDFs of the local Reynolds stress in Hasagawa-Mima [25, 26] and toroidal ITG turbulence models were investigated by Kim *et al.* [27, 28]. In the following, we consider a slightly different ITG model and compute the PDFs of (global) momentum flux and zonal flow formation [29, 30]. Specifically, we model ITG turbulence using the continuity and temperature equation for the ions, assuming Boltzmann electrons, and ignoring the effects of parallel ion motion, magnetic shear, trapped particles, and finite beta on the ITG modes [31]. We incorporate the effect of an imposed poloidal shear flow in the time-evolution equations for the background fluctuations in the form of sheared velocity V_0 . The main governing equations are given by

$$\begin{aligned} & \partial_t n - (\partial_t - \alpha_i \partial_y) \nabla_\perp^2 \phi + \partial_y \phi + [\phi, n] + \nu \nabla^4 \phi \\ & + V_0 \partial_y (1 - \nabla_\perp^2) \phi - \epsilon_n g_i \partial_y (\phi + \tau (n + T_i)) \\ & = [\phi, \nabla_\perp^2 \phi] + \tau [\phi, \nabla_\perp^2 (n + T_i)] + f, \\ & (\partial_t + V_0 \partial_y) T_i - \frac{5}{3} \tau \epsilon_n g_i \partial_y T_i + \left(\eta_i - \frac{2}{3} \right) \partial_y \phi \\ & - \frac{2}{3} (\partial_t + V_0 \partial_y) n = -[\phi, T_i] + \frac{2}{3} [\phi, n]. \end{aligned} \quad (10)$$

Here, f is the forcing, and V_0 is an imposed shear flow. Notations are standard: $[A, B] = (\partial_x A)(\partial_y B) - (\partial_y A)(\partial_x B)$; $n = (L_n/\rho_s) \delta n/n_0$ is the normalized ion particle density; $\phi = (L_n/\rho_s) e \delta \phi/T_e$ is the electrostatic potential; $T_i = (L_n/\rho_s) \delta T_i/T_{i0}$ the ion temperature; $\tau = T_i/T_e$; $\rho_s = c_s/\Omega_{ci}$ where $c_s = \sqrt{T_e/m_i}$; $\Omega_{ci} = eB/m_i c$; ν is collisionality; $L_T = -(d \ln T / dr)^{-1}$, and $L_n = -(d \ln n / dr)^{-1}$; $\eta_i =$

L_n/L_{T_i} , $\epsilon_n = 2L_n/\bar{R}$ where \bar{R} is the major radius; and $\alpha_i = \tau(1 + \eta_i)$. Length scale and time are normalized by ρ_s and L_n/c_s , respectively. The geometrical quantities are calculated in the strong ballooning limit ($\theta = 0$, $g_i(\theta = 0) = 1$, with $\omega_\star = k_y v_\star = \rho_s c_s k_y / L_n$). Physically, the forcing f is envisioned to arise from the instability of toroidal ITG modes due to unfavorable magnetic curvature, or an external particle source.

We assume that a coherent structure responsible for the PDF tails has the spatial profile given by modons propagating with speed U in the local poloidal y direction as $\phi_0(x, y) = \phi_0(x, y - Ut)$ (for example, [26]). Furthermore, we assume a linear relationship between ϕ and T_i as $T_i = \chi \phi$ with

$$\chi = \frac{\eta_i - \frac{2}{3}(1 - U + V_0)}{U - V_0 + \frac{5}{3} \tau \epsilon_n g_i}.$$

The coupled equations (10) then effectively reduce to one equation for ϕ with the nonlinear interaction term $N[\phi]$ in Eq. (7) given by

$$\begin{aligned} N[\phi] = & -(\partial_t - \alpha_i \partial_y) \nabla_\perp^2 \phi + V_0 (1 - \nabla_\perp^2) \phi \\ & + (1 - \epsilon_n g_i \beta) \partial_y \phi - \beta [\phi, \nabla_\perp^2 \phi] + \nu \nabla^4 \phi, \end{aligned} \quad (11)$$

where $\beta = 1 + \tau + \tau \chi$. By substituting Eq. (11) in S_λ and using $\phi = F(t) \phi_0$, we obtain the effective action S_λ as a function of $F(t)$ and $\bar{\phi}(x, t)$. We note that for a nonlinear modon solution to exist, the ITG mode should be linearly unstable (for example, [32]).

4.1 Momentum flux

We first consider the observable to be momentum flux

$$M[\phi] = \langle v_x v_y \rangle = \left\langle -\frac{\partial \phi}{\partial x} \frac{\partial \phi}{\partial y} \right\rangle, \quad (12)$$

where angle brackets $\langle \rangle$ denote spatial average, and compute the PDFs of the momentum flux $M[\phi]$ to take a value of R (that is, $P(R)$).

By substituting Eq. (12) into S_λ Eq. (7) with $\phi = F(t) \phi_0$, and following Sect. 3 Steps I-IV, we obtain the desired PDFs of the momentum flux $P(R)$ as

$$P(R) \sim \exp\{-c_1 R^{3/2}\}, \quad (13)$$

where c_1 is a constant that depends on the profile of the coherent structure (modon) and the values of the physical parameters ($U - V_0$, η_i , τ , etc). Equation (13) clearly shows that the PDF tails are strongly intermittent with exponential scaling $\exp(-cR^{3/2})$. Our prediction thus offers a powerful mechanism for ubiquitous exponential scalings observed experimentally (for example, [10–13]). Notably, exactly the same exponential scaling $\exp(-cR^{3/2})$ of Reynolds stress was reported in [11]. Of particular importance, we find that the PDF is enhanced over the Gaussian prediction $\exp(-cR^2)$, highlighting the importance of intermittency in understanding momentum transport. Similar $\exp(-cR^{3/2})$ was also obtained in the PDFs of local momentum flux and heat flux in Hasagawa-Mima and toroidal

ITG turbulence models [27,28]. These results follow from the fact that (i) the highest nonlinearity in our model is quadratic and (ii) the observable is the second-order moment (momentum flux) [33]. Were it not for a linear relationship between T_i and ϕ , a different exponential scaling would have followed. On the other hand, the constant c_1 depends on the spatial profile of the coherent structure (modons), $U - V_0$, and other physical parameters (η_i , τ , etc.), which is investigated in detail in [30].

4.2 Zonal flow formation

We consider zonal flows, driven by Reynolds stress (momentum flux), as

$$\frac{\partial \phi_{ZF}(t)}{\partial t} = -\langle v_x v_y \rangle. \quad (14)$$

To include the dynamics of zonal given in Eq.(14), we need to introduce the conjugate variable for zonal flows as $\bar{\phi}_{ZF}$. The additional contribution from zonal flows to the action S_λ is then given by

$$\Delta S_\lambda = -i \int dt \bar{\phi}_{ZF}(t) \left(\frac{\partial \phi_{ZF}(t)}{\partial t} + \langle v_x v_y \rangle \right). \quad (15)$$

To compute the PDFs of zonal flows, we consider the observable to be zonal flows

$$M[\phi_{ZF}] = \phi_{ZF}. \quad (16)$$

By incorporating ΔS_λ (Eq. (15)), substituting Eq. (16) into Eq. (7), and following Sect. 3 Steps I-IV, we obtain PDFs of zonal flows to take the value of R (that is, $P(R)$) as follows:

$$P(R) \sim \exp\{-c_2 R^3\}. \quad (17)$$

Here, c_2 is the model-dependent constant that determines the amplitude of the PDFs. The exponential scaling in Eq. (17) again indicates a strong intermittency in the tails. The exact scaling here follows from the fact that (i) the highest nonlinearity in our model is quadratic and (ii) the observable is the first order moment (zonal flow). Note that, for the same reason, a similar $\exp(-cR^3)$ scaling was found in the tails of the PDFs of positive velocity gradients in Burgers turbulence [18]. While the exponential scaling is robust, the amplitude of the PDFs rather sensitively depends on parameter values in the model through the value of the constant c_2 [30, 33]. Similar exponential PDFs are thus expected when the effect of toroidal coupling is incorporated, with the same (quadratic) highest nonlinearity in Eq. (10). The toroidal effect will however change the overall amplitude of PDFs by effectively altering the forcing strength (κ_0).

Note that, in this model, the back reaction of zonal flows is neglected, by assuming an imposed shear flow. Computation of the PDFs in a more consistent model is in progress where zonal flows are treated dynamically by allowing them to modify the evolution of fluctuations. Finally, note that a simplified 1D model for a shear flow

has been proposed in terms of a nonlinear diffusion equation, where a shear flow is driven by a stochastic forcing while damped through a nonlinear diffusion of the form $D(u_x) = \gamma u_x^2$ [34]. Here, $u_x = \partial_x u$; γ is constant. Analysis of this model was recently done by [35].

4.3 Summary

The instanton method predicts exponential PDFs of momentum flux (second moments) and structure formation (first moments) with $\exp(-cR^{3/2})$ and $\exp(-c_2 R^3)$ scalings, respectively. Our theory thus explains similar exponential PDF tails often observed in various tokamaks [11–13]. Furthermore, we can show that PDFs of higher moments such as $\langle n v_x v_y \rangle$ have exponential PDFs that are much more enhanced compared to the Gaussian distribution, possibly explaining the numerical results in [10].

5. Discussions and Conclusion

We presented a statistical theory of turbulence and intermittency that is rather insensitive to the details of a dynamical system and depends on only the highest nonlinear interaction. The method is motivated by various experimental results that show that coherent structures tend to arise from complex, multi-scale interactions in plasmas, manifesting a tendency toward self-organization. These coherent structures are often associated with bursty events, causing a significant transport, such as, for instance, hampering plasma confinement in laboratory plasmas. This empirical fact is built into the instanton method, employed for our study. The predicted scaling is exponential, offering a powerful mechanism to explain similar exponential PDF tails observed in various tokamaks [11–13].

The instanton method is not a new theory; it was originally introduced in quantum field. However, it appears to be a useful technique for examining plasma turbulence, with much scope for further investigation. While the leading order prediction of instantons is limited to exponential PDFs, there is much hope that extension of this method will give more diverse scaling predictions, including the combination of exponential and power-law, power-law, etc that can explain not only the tails but the form of the PDFs near the center. Note that in Burgers turbulence, the left tail of the PDF for the velocity difference due to shocks satisfies a power-law scaling.

The few steps to improve the present predictability of the instanton method include: (i) keep contributions from the perturbations around the instanton (that is, the higher-order corrections in the action and path integral); in other words, incorporate both coherent structures and fluctuations (turbulence); (ii) incorporate contributions from anti-instantons (see Fig. 2), multi-instantons, and multi-structures; (iii) generalize the method to account for a finite-correlation time of the forcing and for non-Gaussian statistics; and (iv) derive consistently the forcing that may arise from some instabilities in a system, rather than taking

it to be given. These improvements are expected to provide a theoretical framework in which a broad range of experimental data, including finite size scaling with power-law PDFs [36], can be understood. Finally, while the exact value of the PDF amplitude requires knowledge of the spatial form of coherent structures (for example, exact nonlinear solutions), a good estimate can be obtained by finding an approximate nonlinear solution, or by empirically constructing it from numerical or experimental results even if the exact form may not be available.

Acknowledgments

This research was supported by the Engineering Physical Science Research Council (EPSRC) grant EP/D064317/1.

- [1] S. Zweben, *Phys. Fluids* **28**, 974 (1985).
- [2] M. Endler *et al.* and ASDEX team, *Nucl. Fusion* **35**, 1307 (1995).
- [3] R.A. Moyer *et al.*, *Plasma Phys. Control. Fusion* **38**, 1273 (1996).
- [4] D.A. Russell, J.R. Myra and D.A. D'Ippolito, *Phys. Plasmas* **14**, 102307 (2007).
- [5] O.E. Garcia *et al.*, *Nucl. Fusion* **47**, 667 (2007).
- [6] D.A. Russell *et al.*, *Phys. Rev. Lett.* **93**, 265001 (2004).
- [7] B.D. Scott, *Plasma Phys. Control. Fusion* **49**, S25 (2007).
- [8] X.Q. Xu *et al.*, *Phys. Plasmas* **10**, 1773 (2003).
- [9] S.I. Krasheninnikov, D.A. D'Ippolito and J.R. Myra, *J. Plasma Phys.* **74**, 679 (2008).
- [10] J.R. Myra, D.A. Russell and D.A. D'Ippolito, *Phys. Plasmas* **15**, 032304 (2008).
- [11] Z. Yan, G.R. Tynan, J.H. Yu *et al.*, On the statistical properties of turbulent Reynolds stress, 49th APSDPP November 12-16, 2007, Orlando, Fl. USA.
- [12] S.J. Zweben *et al.*, *Plasma Phys. Control. Fusion*, **49**, S1 (2007).
- [13] F. Sattin *et al.*, *Plasma Phys. Control. Fusion*, **48**, 1033 (2006).
- [14] E. Kim and P.H. Diamond, *Phys. Rev. Lett.* **90**, 185006 (2003).
- [15] K. Itoh *et al.*, *J. Plasma Fusion Res.* **79**, 608 (2003).
- [16] S. Coleman, *Aspects of Symmetry* (Cambridge University Press, Cambridge, 1985).
- [17] G. 't Hooft, *Phys. Rev. Lett.* **37**, 8 (1976).
- [18] V. Gurarie and A. Migdal, *Phys. Rev. E* **54**, 4908 (1996).
- [19] G. Falkovich *et al.*, *Phys. Rev. E* **54**, 4896 (1996).
- [20] E. Balkovsky *et al.*, *Phys. Rev. Lett.* **78**, 1452 (1997).
- [21] J. Fleischer and P.H. Diamond, *Phys. Lett. A* **283**, 237 (2001).
- [22] H.W. Wyld, *Ann. Phys.* **14**, 143 (1961).
- [23] J. Zinn-Justin, *Quantum Field Theory and Critical Phenomena* (Clarendon Press, Oxford, 1989).
- [24] P.C. Martin, E.D. Siggia and H.A. Rose, *Phys. Rev. E* **8**, 423 (1973).
- [25] A. Hasegawa and K. Mima, *Phys. Rev. Lett.* **39**, 205 (1977).
- [26] W. Horton, *Rev. Mod. Phys.* **71**, 735 (1999).
- [27] E. Kim and P.H. Diamond, *Phys. Plasmas* **9**, 71 (2002); *Phys. Rev. Lett.* **88**, 225002 (2002).
- [28] E. Kim *et al.*, *Nucl. Fusion* **43**, 961 (2003).
- [29] J. Anderson and E. Kim, *Phys. Plasmas* **15**, 052306 (2008).
- [30] J. Anderson and E. Kim, *Phys. Plasmas* **15**, 082312 (2008).
- [31] J. Anderson, H. Nordman, R. Singh *et al.*, *Phys. Plasmas* **9**, 4500 (2002).
- [32] B.G. Hong, F. Romanelli and M. Ottaviani, *Phys. Fluids B* **3**, 615 (1991).
- [33] E. Kim and J. Anderson, *Phys. Plasmas* **15**, 114506 (2008).
- [34] H.-L. Liu, *J. Atmospheric Sci.* **64**, 580 (2007).
- [35] E. Kim, H.-L. Liu and J. Anderson, *Phys. Plasmas* **16**, 052304 (2009).
- [36] C. Hildago *et al.*, *New J. Phys.* **4**, 51 (2002).